An Adaptive-Harvest-Then-Transmit Protocol for Wireless Powered Communications: Multiple Antennas System and Performance Analysis

Nguyen Xuan Xinh[1,2], Dinh-Thuan Do[1,2]
[1]Wireless Communications Research Group (WiCOM), Ton Duc Thang University, Ho Chi Minh City, Vietnam
[2]Faculty of Electrical & Electronics Engineering, Ton Duc Thang University, Ho Chi Minh City, Vietnam
[e-mail: xuanxinhspkt@gmail.com; dodinhthuan@tdt.edu.vn]
*Corresponding author: Dinh- Thuan Do

Received May 21, 2016; revised November 25, 2016; revised Janaury 23, 2017; accepted February 14, 2017; published April 30, 2017

Abstract

This paper investigates a protocol so-called Adaptive Harvest Then Transmit (AHTT) for wireless powered communication networks (WPCNs) in multiple-input single-output (MISO) downlink systems, which assists in transmitting signals from a multi-antenna transmitter to a single-antenna receiver. Particularly, the power constrained relay is supplied with power by utilizing radio frequency (RF) signals from the source. In order to take advantage of multiple antennas, two different linear processing schemes, including Maximum Ratio Combining (MRC) and Selection Combination (SC) are studied. The system outage capacity and ergodic capacity are evaluated for performance analysis. Furthermore, the optimal power allocation is also considered. Our numerical and simulation results prove that the implementation of multiple antennas helps boost the energy harvesting capability. Therefore, this paper puts forward a new way to the energy efficiency (EE) enhancement, which contributes to better system performance.

Keywords: Wireless powered communications (WPC), multiple antennas, multiple-input single-output, multiple antennas, power allocation

This research was funded by Foundation for Science and Technology Development of Ton Duc Thang University (FOSTECT), website: http://fostect.tdt.edu.vn, under Grant FOSTECT.2016.BR.21

https://doi.org/10.3837/tiis.2017.04.004 **ISSN : 1976-7277**

1. Introduction

During the last ten years, a lot of research interest has been taken in the field of transmitting energy without using wires, so radio-frequency (RF) radiation has become a possible source for energy harvesting (EH). These days, it is viable to transmit energy wirelessly efficiently over near distances. Additionally, wireless nodes in popular networks such as cellular networks can harvest RF signals to supply their transmissions, which have been presented in recent works ([1-2] and, references therein). Wireless networks could be provided with energy supplies by wireless power transfer (WPT), which is a new potential candidate for EH. In fact, it is also implementable by different technologies like magnetic resonate coupling, inductive coupling and electromagnetic (EM) radiation for short-/mid-/long-range applications, respectively. In reality, RF-enabled WPT and EM are tested in either cellular networks or wireless sensor networks (WSNs). Simultaneous wireless information and power transfer (SWIPT) is strived by a unified research, because radio signals are able to carry both energy and information simultaneously. In particular, a multiple-input multiple-output (MIMO) wireless broadcast system is studied, which helps one receiver the harvested energy and another receiver understand data separately. Besides that, multiple antennas are equipped for all receivers and transmitters. In practice, the exploitation of EH function can be conducted in either transmit or receive side [3-9]. For the EH receiver, the management of information decoding has been developed, in which EH scheduling and the transmit power allocation have been taken into consideration in cooperative networks in [3-6] and wireless sensor networks in [7], respectively. Additionally, multi-antenna based energy beamforming was proposed in [8, 9].

In order to take advantage of MIMO, where before obtaining energy beamforming gains, the energy-bearing signals are processed at the multiple transmit antennas. As example, massive MIMO models (e.g [10 – 13]) were considered to be appropriate for RF EH, where there are an huge number of antennas equipped at the energy transmitter to achieve enormous beamforming gains. Consequently, they help enhance the end-to-end EE significantly. In terms of multiple-input single output (MISO) channels, the investigations into the optimal beamforming designs for SWIPT systems with/without secrecy constraint were conducted in [14, 15], and an optimal transmission strategy to maximize the system throughput of MISO interference channels was studied in [16]. Additionally, the application of RF energy transfer techniques in cognitive radio networks with multiple antennas at the secondary transmitter was considered in [17]. Very recently, the authors in [18] studied a WPCN equipped with one multi-antenna access point (AP) and one single-antenna user. Considering Harvest-Then-Transmit (HTT) protocol implemented in the network, the optimal EH time was derived for both delay-constrained and delay-tolerant transmission modes. It is necessary to notice that most of the previous works focus on the point-to-point communication systems.

In order to make sure that the information receivers in SWIPT can receive the message surreptitiously even when being eavesdropped by any individual energy receivers, multiple-input single-output (MISO) secrecy communication schemes were studied in [14], in which the transmitter side is able to experience perfect channel state information (CSI) of the information receivers and energy receivers. In [19], an impactful SWIPT scheme for boosting secrecy rate has been taken into consideration under the impact of external eavesdroppers. It is clear that robust designs for SWIPT have also been investigated in [20]. Radio transmission is so weak that it can be attacked from unexpected eavesdroppers, due to broadcast nature of

radio propagation and inherent randomness of wireless channel, which use higher signal-to-noise ratio supplied at eavesdroppers. Communication security with SWIPT in MISO channels was studied in [21, 22]. Specifically, the aforementioned tradeoff is researched in MIMO systems for two information and power transfer architectures, i.e., time-switching and power-splitting, for both perfect [9] and imperfect [22] channel state information (CSI), respectively. Another method was considered in [23], where the trade-off between the information and the energy transfer is investigated in a multi-user network under two different constraints, i.e., a constraint shown with respect to secrecy rate for the former and amount of which is harvested at the receiver for the latter.

In addition, [18] considers EH time to obtain fixed duration and which is similar to [3-9], [18], this process, which leads to variation of the harvested energy at users based on channel gain, does not enable presetting energy at user nodes. Hence, it is still an open problem to designing a protocol which allows energy to be adaptationally harvested at user nodes. In this paper, we conduct investigations into wireless powered network used Adaptive Harvest Then Transmit (AHTT) protocol. There are several main contributions which are summarized below.

- An up-to-date protocol for WPCNs, namely AHTT is proposed, in which EH time is adaptively switched depending on the calculated channel information between the AP and the user node.
- The delay-constrained and delay-tolerant transmission schemes for both Maximum Ratio Combining (MRC) and Selection Combining SC receiving methods at AP node are taken into consideration, an then we obtain a closed-form expression for the average throughput of the proposed protocol over independent and identical distribution (i.i.d) Rayleigh fading channels.
- An optimal power transmission at the user node in instantaneous transmission mode is derived analytically.
- To show the advantages of our proposed protocol, we compare the system performance with results presented in [18]. Numerical and simulation results are presented to corroborate the theoretical comparison and the superiority of the AHTT scheme.

The remainder of the paper is organized as follows. Section 2 presents the system model and illustrates the wireless powered protocol. The system performance is analyzed in Section 3 while Section 4 assesses the throughput performance by simulations. Eventually, the conclusion of this paper is described in Section 5.

2. System model and protocol description

2.1 System description

As illustrated in **Fig. 1,** a MISO system is considered, in which it consists of a hybrid access point (H-AP) with multiple antennas and a single-antenna user node (U node). The H-AP is equipped with N antennas, and functions like a conventional AP, (i.e, exchanging data to/from users). Nevertheless, wirelessly harvested power is supplied for the user. In terms of frame-based transmission, there are three phases, including the uplink channel estimation, the downlink wireless energy transmission and the uplink wireless information transmission. In the first stage, the user utilizes a part of the harvested energy to transfer pilots, while the uplink

and downlink channels are estimated and obtained by exploiting channel reciprocity, respectively. Afterwards, the H-AP uses the obtained channel calculation to transmit energy to the user in the downlink via energy beamforming. Eventually, a portion of the harvested energy is used to send data to the H-AP at the same time in the uplink.

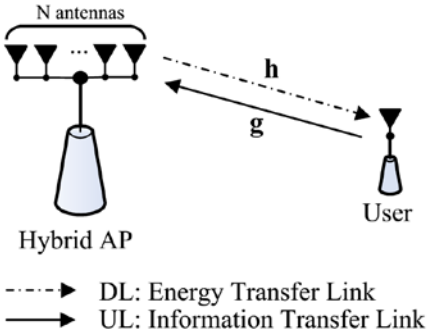

Fig. 1. Wireless powered communication with multi-antenna system.

2.2 AHTT protocol

A time switching scheme for SWIPT networks is implemented in this system model. In this protocol, the system communication in a time block, T , where in each block, it can be divided into two sub-blocks, i.e. *(i) Downlink (DL) energy* and *(ii) Uplink (UL) information*. In this proposed protocol, the transmit power at the user denoted by P_U is set to a fixed value. Therefore, it only harvests enough energy in each block for its preset power. Based on the available parameters, such as channel power gains, transmitted power at H-AP and the distance between the user and H-AP, which can help calculate exactly the amount of time for EH.

In comparison with Harvest Then Transmit (HTT) strategy, which is widely used in previous works [2-4], [6-8], [10-14], the proposed protocol allows the user node to preset its harvested energy and transmit power that is helpful when WPC system operates in the low-power regime, such as cognitive radio networks [13]. Nevertheless, the HTT protocol in [14] has a fixed DL time for each time block with the values of P_U fluctuating based on the random DL channel gains. Meanwhile, our proposed AHTT protocol permits the user node to change time of DL stage to satisfy a preset transmit power at the user node. Consequently, the user node transmits at a constant power level, meaning that the transmission scheme design has been significanly simplified and the required dynamic region of the power amplifier at user node has been smaller compared to model illustrated in [24]. Although AHTT requires the knowledge of instantaneous CSI and some system parameters to optimaze the system performance (i.e, instantaneous transmission mode in Sec. 3.2), which help the user node use more plot sequences, the optimal transmission power can be calculated by using static CSI by exhaustive search method (see Sec. 3.3 and Sec. 3.4).

Channel assumptions: in this EH strategy, the channels are assumed as follows

- The channels have a Rayleigh-fading distributed, which keeps constant over the block time T and varies independently and identically from one block to the other.
- Full CSI is assumed at both AP and U node.

- The receiver side CSI is assumed to be perfect, which is in line with the previous work in [14-18]. We assume a quasi-static channel model with perfect CSI at the AP.

2.3 Signal Model

With CSI available at AP, the maximum ratio transmission (MRT) is used with beamforming vector to achieve optimal transmission scheme as in [9, 18], with $\|\mathbf{w}_i\|=1$

$$\mathbf{w}_i = \frac{\mathbf{h}_i}{\|\mathbf{h}_i\|}, \tag{1}$$

where $\|.\|$ denotes the Euclidean norm of a matrix. The harvested signal at U node in the DL stage is thus given by

$$\mathbf{y}_{U,i} = \frac{\|\mathbf{h}_i \mathbf{w}_i\|}{\sqrt{d^m}}\sqrt{P_{AP}}\,x_i + \mathbf{n}_{U,i}. \tag{2}$$

In (2), x_i is the transmitted symbol at ith time slot from the source, $\mathbf{h}_i$ is the $N\times 1$ channel vector for the DL link at the block time i th, $\mathbf{n}_{U,i}$ is the additive white Gaussian noise (AWGN) with zero mean and variance matrix $\sigma_U^2\mathbf{I}_N$, d presents the distance between nodes and m is the path loss exponent.

Hence, the harvested energy at the user node in a part of time is determined after eliminating the noise as [18]

$$\mathcal{E}_{U,i} = \eta\alpha_i T\frac{P_{AP}\|\mathbf{h}_i\|^2}{d^m}, \tag{3}$$

where $0\le\eta\le 1$ is energy conversion efficiency at the energy receiver and it depends on the rectifier and the EH circuitry, α_i is the time duration allocated for wireless power transfer stage, and T (sec) is the block time.

In AHTT protocol, the power transmission at user node is denoted as P_U with a fixed value, i.e.. Hence, the energy used to communication can be expressed as

$$\mathcal{E}_{U,i} = P_U\left(1-\alpha_i\right)T. \tag{4}$$

From (3) and(4), the allocated fraction of time, α_i, for power transfer in i th block time can be written as

$$\alpha_i = \frac{P_U d^m}{\eta P_{AP}\|\mathbf{h}_i\|^2 + P_U d^m}. \tag{1}$$

Remark 1: The user node is be able to harvest then transmit with normal power of P_U, in each time block. In particular, in(5), $P_U d^m$ existes in both in the numerator and in the denominator. This illustrates that α_i is always less than 1, meaning that the user is capable of harvesting the required amount of energy. Hence, the user node enables UL information with P_U to AP node in each block.

In UL information phase, the user node uses the harvested energy completely in the DL phase to transmit information to AP node. Thus, the received signal at AP node is given by

$$\mathbf{y}_{AP,i} = \frac{\mathbf{g}_i}{\sqrt{d^m}}\sqrt{P_U}\,x_i + \mathbf{n}_{AP,i}, \tag{6}$$

where $\mathbf{g}_i$ is the $1\times N$ channel vector for the UL link in the block time ith, $\mathbf{n}_{AP,i}$ is the AWGN at AP node with variance matrix $\sigma^2_{AP,i}\mathbf{I}_N$.

3. Performance Analysis of Proposed AHTT Protocol

The system throughput performance in instantaneous, delay-constrained and delay-tolerant transmission modes are studied in this section. We will evaluate them with regard to outage probability and ergodic capacity. The preset optimal transmit power at user is also evaluated, which contributes to the achievement of optimal system throughput in these considered transmission modes.

3.1 SNR analysis

3.1.1 MRC model

The maximum ratio combing (MRC) technique is assumed to perform at the AP to mix the received signal at the AP node by the received weight vector $\mathbf{w}_{R,i} = \mathbf{g}_i^T / \|\mathbf{g}_i\|$. Here, $\mathbf{x}^T$ is the transpose transformation of matrix $\mathbf{x}$. Thus, the resulting signal at the receiver can be written as $y_{MRC,i} = \mathbf{w}_{R,i}\mathbf{y}_{AP,i} = \sqrt{P_U d^{-m}}\,\|\mathbf{g}_i\|x_i + \mathbf{w}_{R,i}\mathbf{n}_{AP,i}$. To this end, the achieved SNR using MRC scheme is given as

$$\gamma_{MRC,i} = \frac{P_U \|\mathbf{g}_i\|^2}{d^m \sigma^2_{AP,i}}. \tag{7}$$

3.1.2 SC model

In SC scheme, at the receiver, the best instantaneous UL gain is chosen to decode the transmitted signal. Therefore, according to both the received signal at AP like and SC method, the received signal can be written as $y_{SC,i} = \max\{\mathbf{y}_{AP,i}\} = \sqrt{P_U d^{-m}}\,\max\{|\mathbf{g}_i|^2\}x_i + n_{AP,i}$. Thus, since the SC method is utilized at AP node, the instantaneous SNR at AP node is given by

$$\gamma_{SC,i} = \frac{P_U \max\{|\mathbf{g}_i|^2\}}{d^m \sigma^2_{AP,i}}. \tag{8}$$

3.2 Instantaneous transmission mode

In this transmission mode, the system performance is optimized in each block with available instantaneous CSI. The instantaneous throughput of WPC systems at *i*th time block can thus be determined as

$$C_{\Re,i} = (1-\alpha_i)\log_2(1+\gamma_{\Re,i}), \tag{9}$$

where $\Re \in \{MRC,\ SC\}$.

The optimal transmit power at the user node can be formulated as

$$\begin{aligned} P_{U,i}^{opt} &= \arg\max\left\{C_{\Re,i}\left(P_{U,i}\right)\right\}, \\ &\text{s.t } 0 \le P_{U,i}. \end{aligned} \tag{10}$$

3.2.1 MRC model

Substituting (5) and (7) into (9), the instantaneous throughput of MRC technique is the function of user's transmit power as

$$C_{MRC,i} = \frac{\eta P_{AP,i}\left\|\mathbf{h}_i\right\|^2}{\eta P_{AP,i}\left\|\mathbf{h}_i\right\|^2 + P_{U,i}d^m}\log_2\left(1+\frac{P_{U,i}\left\|\mathbf{g}_i\right\|^2}{d^m\sigma_{AP}^2}\right). \tag{11}$$

Proposition 1: The maximum instantaneous throughput can be computed related to the optimal power allocation for with MRC technique at the receiver is given by

$$P_{U,i}^{opt} = \frac{Nd^m\sigma_{AP,i}^2}{\left\|\mathbf{g}_i\right\|^2}\left\{\exp\left[W\left(\frac{\eta P_{AP,i}\left\|\mathbf{h}_i\right\|^2\left\|\mathbf{g}_i\right\|^2}{ed^{2m}\sigma_{AP,i}^2}-\frac{1}{e}\right)+1\right]-1\right\}, \tag{12}$$

where $e \approx 2.718$ is exponent constancy and $W(x)$ is the Lambert W function with a solution of $W(\Omega)=\omega$ is $\omega\exp(\omega)=\Omega$.

Proof : see appendix A.

3.2.2 SC model

Substituting (5) and (8) into (9), the instantaneous throughput of SC technique is computed as

$$C_{SC,i} = \frac{\eta P_{AP,i}\left\|\mathbf{h}_i\right\|^2}{\eta P_{AP,i}\left\|\mathbf{h}_i\right\|^2 + P_{U,i}d^m}\times\log_2\left(1+\frac{P_{U,i}\max\left\{\left|\mathbf{g}_i\right|^2\right\}}{d^m\sigma_{AP}^2}\right). \tag{13}$$

Proposition 2: The optimal power allocation for maximum instantaneous throughput with SC scheme is derived as

$$P_{U,i}^{opt} = \frac{d^m\sigma_{AP}^2}{\max\left\{\left|\mathbf{g}_i\right|^2\right\}}\left\{\exp\left[\mathrm{W}\left(\frac{\eta P_{AP,i}\left\|\mathbf{h}_i\right\|^2\max\left(\left|\mathbf{g}_i\right|^2\right)}{ed^{2m}\sigma_{AP}^2}-\frac{1}{e}\right)+1\right]-1\right\}, \tag{14}$$

where e is constant and W function is defined in Proposition 1 below.

Proof : the proof is similar to Proposition 1.

3.3 Delay-Constrained transmission Mode

In the delay-constrained transmission mode, the length of the code will be divided into small packages, in which their size is worse compared to the transmission block. Therefore, the received signal is processed block by block at the AP node. In this mode, the system performance is evaluated in terms of outage throughput. The system outage throughput at the time slot, *i*th, is the function of outage probability and the EH duration, which is expressed by

$$\tau_i = R\left(1-OP_i\right)\left(1-\alpha_i\right). \tag{15}$$

Next, the average outage throughput of system is determined by operative expectation as

$$\tau = \mathbf{E}\left\{\tau_i\right\} = \mathbf{E}\left\{R\left(1-OP_i\right)\left(1-\alpha_i\right)\right\}, \tag{16}$$

in which $\mathbf{E}\{.\}$ is the expectation function and R factor in (15) is the fixed transmission rate of the user node.

It is noted that the outage probability at ith time slot, OP_i, is defined as

$$OP_i = \Pr\left\{\gamma_i < \gamma_o\right\}, \tag{17}$$

with γ_i is the SNR at AP node, which is determined in (7) for MRC technique and in (8) for using SC technique at terminal node, and $\gamma_o = 2^R - 1$ is called as the threshold SNR for decoding the exact signal and R is the transmission rate.

The optimal value of the transmit power for maximizing throughput through the function below

$$\begin{aligned} P_U^{opt} &= \arg\max\left\{\tau\left(P_U\right)\right\}, \\ &\text{s.t } 0 \le P_U. \end{aligned} \tag{18}$$

Thus, the rest of the main work is to evaluate the exact outage throughput of the system. Now, we are studying that.

3.3.1 MRC model

Substituting (5) and (7) into (15), the outage throughput of MRC scheme in block time ith is given as

$$\tau_{MRC,i} = R \times \Pr\left\{\frac{P_U \left\|\mathbf{g}_i\right\|^2}{d^m \sigma_{AP,i}^2} > \gamma_o\right\}\left(1 - \frac{P_U d^m}{\eta P_{AP}\left\|\mathbf{h}_i\right\|^2 + P_U d^m}\right). \tag{19}$$

Proposition 3: The outage throughput of wireless powered communication networks with AHTT EH protocol in case of i.i.d channel and MRC receiver is given by

$$\begin{aligned} \tau_{MRC} = R \times N &\left(\frac{P_U d^m}{\eta P_{AP}\lambda_h}\right)^N \exp\left(\frac{P_U d^m}{\eta P_{AP}\lambda_h}\right)\Gamma\left(-N, \frac{P_U d^m}{\eta P_{AP}\lambda_h}\right) \\ &\times \exp\left(-\frac{d^m \sigma_{AP,i}^2 \gamma_o}{P_U \lambda_g}\right)\sum_{i=1}^{N}\frac{1}{(i-1)!}\left(\frac{d^m \sigma_{AP,i}^2 \gamma_o}{P_U \lambda_g}\right)^{i-1}, \end{aligned} \tag{20}$$

where $\Gamma(a,b)$ is is upper incomplete Gamma function given by (Eq. (8.350)) in [25].

Proof: **please refer appendix B.3.3.2 SC model**

Substituting (5) and (8) into (15), the outage throughput of SC scheme in block time ith is given as

$$\tau_{SC,i} = R \times \Pr\left\{\frac{P_U \max\left(\left|\mathbf{g}_i\right|^2\right)}{d^m \sigma_{AP,i}^2} > \gamma_o\right\}\left(1 - \frac{P_U d^m}{\eta P_{AP}\left\|\mathbf{h}_i\right\|^2 + P_U d^m}\right). \tag{21}$$

Proposition 4: The outage throughput of SC scheme over i.i.d channels for wireless powered communication system is given by

$$\tau^{SC} = N\left(N+1\right)R\times\left[1-\sum_{p=0}^{N}\binom{N}{p}\left(-1\right)^{p}\exp\left(-\frac{pd^{m}\sigma_{AP}^{2}\gamma_{o}}{P_{U}\lambda_{g}}\right)\right] \times\left(\frac{P_{U}d^{m}}{\eta P_{AP}\lambda_{h}}\right)^{N}\exp\left(\frac{P_{U}d^{m}}{\eta P_{AP}\lambda_{h}}\right)\Gamma\left(-N,\frac{P_{U}d^{m}}{\eta P_{AP}\lambda_{h}}\right). \tag{22}$$

Proof*:* please refer appendix C.

Substituting (20) (or (22)) into (18), the optimal transmit power, which optimizes the system throughput for MRC receiver (or SC receiver) is derived. However, due to the complexity of the involved expression, a closed-from solution is not possible. Instead of addressing analyitcal expressions in this work, the optimal value is numerically evaluated using the simulated method in Matlab software.

3.4 Delay tolerant transmission mode

The AP is believed that it can store the received information blocks in buffer unit and experience the inhibition for decoding the received signal. Hence, the code length can be kept large in comparison with transmission block time. After that, the average throughput can be determined by evaluating the ergodic capacity at AP [18]. In this mode, we evaluate the system performance in terms of ergodic throughput, and the ergodic throughput at any ith block times can be expressed as

$$C_{i} = \left(1-\alpha_{i}\right)\log_{2}\left(1+\gamma_{i}\right). \tag{23}$$

Then, using the statistical expectation, the average throughput is given by

$$C = \mathbf{E}\left\{C_{i}\right\} = \mathbf{E}\left\{\left(1-\alpha_{i}\right)\log_{2}\left(1+\gamma_{i}\right)\right\}. \tag{24}$$

The optimal value of transmit power at user node, P_{U}^{opt}, can be derived by resolving the below expression as

$$P_{U}^{opt} = \arg\max\left\{C\left(P_{U}\right)\right\}, \quad \text{s.t } 0 \le P_{U}. \tag{25}$$

Therefore, the exact ergodic throughput of the system will be addressed in the next section.

3.4.1 MRC model

Based on (5) and (7) the capacity throughput of MRC system in (24) can be rewritten as

$$C_{MRC} = \mathbf{E}_{\left\|\mathbf{h}_{i}\right\|^{2}}\left\{1-\frac{P_{U}d^{m}}{\eta P_{AP}\left\|\mathbf{h}_{i}\right\|^{2}+P_{U}d^{m}}\right\}\times\mathbf{E}_{\left\|\mathbf{g}_{i}\right\|^{2}}\left\{\log_{2}\left(1+\frac{P_{U}\left\|\mathbf{g}_{i}\right\|^{2}}{d^{m}\sigma_{AP,i}^{2}}\right)\right\}. \tag{26}$$

Proposition 5: The ergodic throughput in case i.i.d channel and MRC receiver is given by

$$C_{MRC} = \frac{N}{\ln(2)}\exp\left(\frac{d^m\sigma_{AP}^2}{P_U\lambda}\right)\sum_{k=1}^{N}\mathrm{E}_k\left(\frac{d^m\sigma_{AP}^2}{P_U\lambda}\right) \times\left(\frac{P_U d^m}{\eta P_{AP}\lambda_h}\right)^N \exp\left(\frac{P_U d^m}{\eta P_{AP}\lambda_h}\right)\Gamma\left(-N,\frac{P_U d^m}{\eta P_{AP}\lambda_h}\right), \tag{27}$$

where $\mathrm{E}_n(z)=\int_1^\infty e^{-zt}/t^n dt$ is the is the exponential integral function given by (Eq. (5.1.4)) in [26].

***Proof**:* in , the first term is given in , the second element is determined as below

$$D = \mathbf{E}_{\|\mathbf{g}_i\|^2}\left\{\log_2\left(1+\frac{P_U\|\mathbf{g}_i\|^2}{Nd^m\sigma_{AP,i}^2}\right)\right\} = \int_0^\infty \log_2\left(1+\frac{P_U x}{d^m\sigma_{AP}^2}\right) f_{\|\mathbf{g}_i\|^2}(x)dx$$
$$= \frac{1}{(N-1)!\lambda^N}\int_0^\infty x^{N-1}\exp\left(\frac{-x}{\lambda}\right)\log_2\left(1+\frac{P_U x}{d^m\sigma_{AP}^2}\right)dx. \tag{28}$$

Then, with the help of the following identity

$$\int_0^\infty y^{a-1}e^{-by}\ln(1+y)dy = \frac{\Gamma(a)e^b}{b^a}\sum\nolimits_{n=1}^{a}\mathrm{E}_n(b). \tag{29}$$

Then, we can rewrite (28) as

$$D = \frac{1}{\ln(2)}\exp\left(\frac{d^m\sigma_{AP}^2}{P_U\lambda}\right)\sum_{k=1}^{N}\mathrm{E}_k\left(\frac{d^m\sigma_{AP}^2}{P_U\lambda}\right). \tag{30}$$

Finally, substituting (43) and (30) into (26), we achieve the proposition 5. This is end of the proof.

3.4.2 SC model

According to (5) and (8), the system throughput in (24) can be rewritten as

$$C_{SC} = \mathbf{E}_{\|\mathbf{h}_i\|^2}\left\{1-\frac{P_U d^m}{\eta P_{AP}\|\mathbf{h}_i\|^2+P_U d^m}\right\}\times\mathbf{E}_{\max\left\{|\mathbf{g}_i|^2\right\}}\left\{\log_2\left(1+\frac{P_U\max\left\{|\mathbf{g}_i|^2\right\}}{d^m\sigma_{AP,i}^2}\right)\right\}. \tag{31}$$

Proposition 6: The ergodic throughput of SC scheme in delay-tolerant transmission mode over i.i.d channels is determined as

$$\tau_{SC} = N\times\left\{\sum_{k=1}^{N}\binom{N-1}{k-1}\left(\frac{-1}{k}\right)^{k-1}\exp\left(-\frac{kd^m\sigma_{AP}^2}{P_U\lambda_g}\right)\mathrm{E}_1\left(\frac{kd^m\sigma_{AP}^2}{P_U\lambda_g}\right)\right\} \times\left(\frac{P_U d^m}{\eta P_{AP}\lambda_h}\right)^N \exp\left(\frac{P_U d^m}{\eta P_{AP}\lambda_h}\right)\Gamma\left(-N,\frac{P_U d^m}{\eta P_{AP}\lambda_h}\right). \tag{32}$$

***Proof**:* the second component in (31) is determined as

$$\begin{aligned} F &= \mathbf{E}_z\left\{\log_2\left(1+\frac{P_U z}{d^m\sigma_{AP,i}^2}\right)\right\} \\ &= \frac{N}{\lambda}\sum_{k=1}^{N}\binom{N-1}{k-1}(-1)^{k-1}\int_0^{\infty}\exp\left(\frac{-kx}{\lambda}\right)\log_2\left(1+\frac{P_U x}{d^m\sigma_{AP}^2}\right)dx \\ &= N\sum_{k=1}^{N}\binom{N-1}{k-1}\frac{(-1)^{k-1}}{k}\times\exp\left(-\frac{kd^m\sigma_{AP}^2}{P_U\lambda}\right)\mathrm{E}_1\left(\frac{kd^m\sigma_{AP}^2}{P_U\lambda}\right). \end{aligned} \tag{33}$$

where $z \triangleq \max\left\{\left|\mathbf{g}_i\right|^2\right\}$ and the last integral is derived by using (Eq. 4.377.2) in [25]. Finally, by substituting (33) and (43) into (31), the proposition 6 can be derived. This completes the proof.

4. Numerical Result and Discussion

In this section, simulation results are provided to prove the derived analytical results. The impact of the transmit power of AP, the number of antennas, and the installed power at user node on the system throughput is investigated. In all following simulations, we set the distance between the AP and user $d=1$, the path loss exponent $m=3$, the noise power $\sigma_{AP}^2=-5$ (dB), transmit power at AP node $P_{AP}=10$ (dB), the energy efficiency $\eta=0.8$, and the user's transmission rate R = 3 (bps) in the delay-constrained mode.

4.1 Throughput versus transmission power of user experiment

At first, the impact of user's transmit power on the instantaneous throughput of different receiving schemes is taken into consideration. **Fig. 2** shows the instantaneous throughput versus transmit power at user node for different combination algorithms at receiver of MISO system. In this experiment, we simulate with $\left|\mathbf{h}\right|^2=\left[1.0,\ 1.1,\ 0.7,\ 0.5\right]$ and $\left|\mathbf{g}\right|^2=\left[0.7,\ 2.2,\ 0.5,\ 1.0\right]$. The highest level of instantaneous throughput can be seen at the transmit power at user, at approximately 4 (dB) when $P_{AP}=8$ (dB) and around 9 (dB) when $P_{AP}=15$ (dB) (see **Table 1** for more detail). It is clear that the MRC scheme achieves higher throughput than the SC scheme over the entire range of the transmit power of user node.

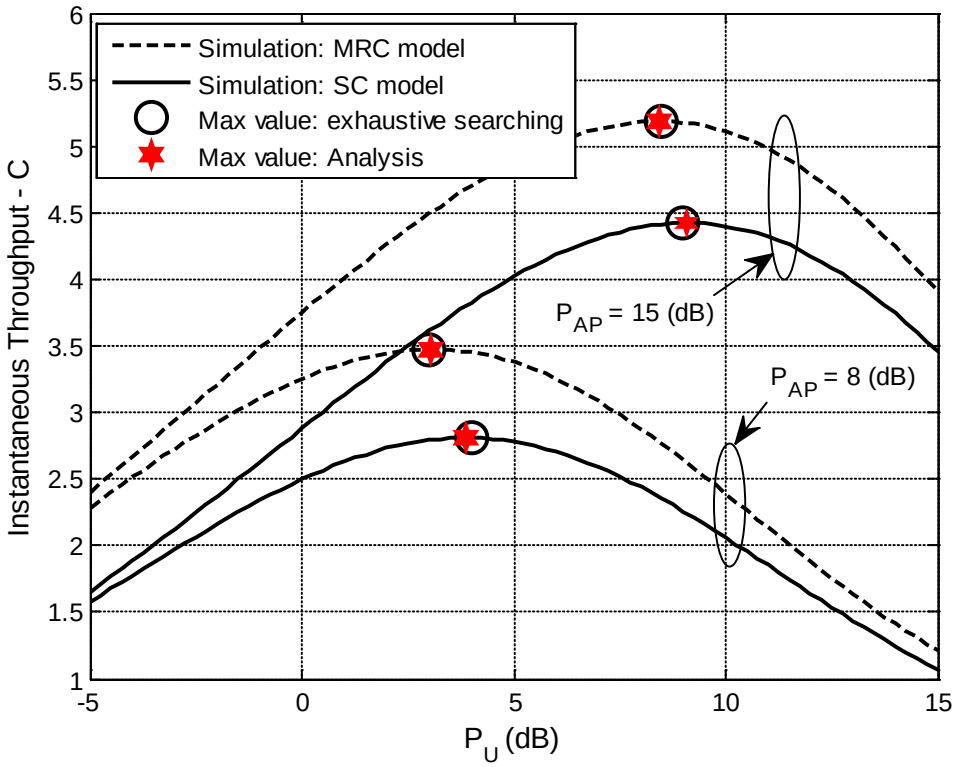

Fig. 2. Instantaneous throughput versus transmit power with different combination methods for delay constrained mode.

Table 1. the optimal value of user transmission power and respective instantaneous throughput in instantaneous transmission mode.

	$P_{AP} = 8$ (dB)		$P_{AP} = 15$ (dB)	
	P_U^{Opt} (dB)	C^{Opt} (bps/Hz)	P_U^{Opt} (dB)	C^{Opt} (bps/Hz)
MRC model	3.00	3.47	8.50	5.18
SC model	4.00	2.81	9.00	4.42

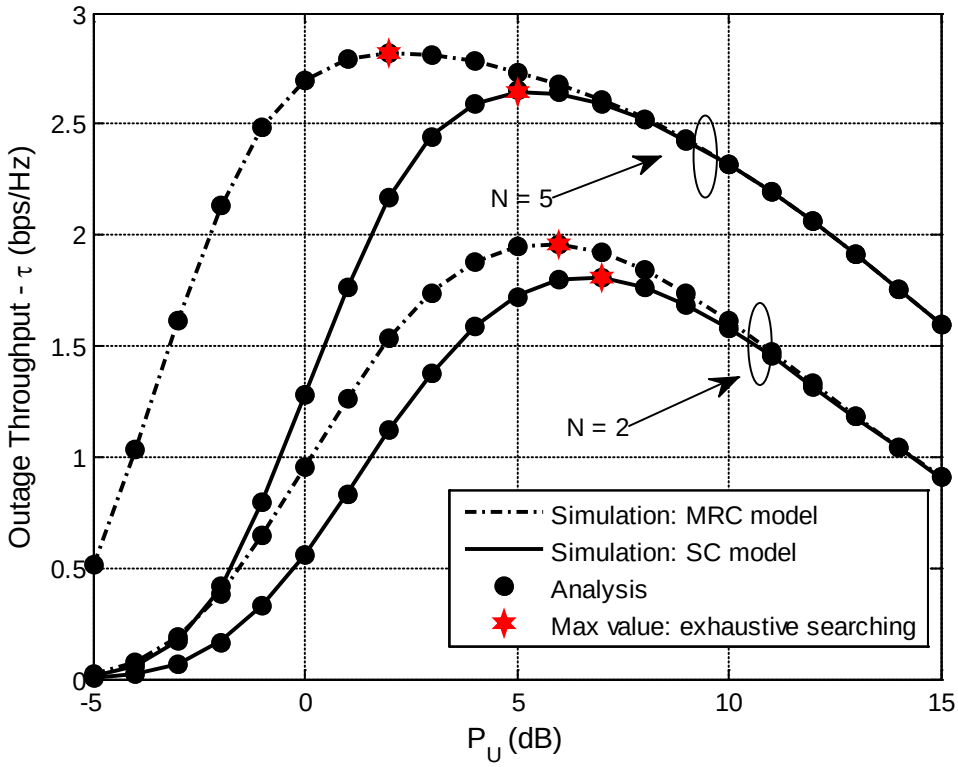

Fig. 3. Outage throughput versus transmit power with different combination methods and different number of antenna at AP, i.e $N \in (\ ,\ 5)$ and, $P_{AP} = 10$ (dB).

Table 2. the optimal value of user transmission power and respective outage throughput in delay-constrained transmission mode.

	$N = 2$		$N = 5$	
	P_U^{Opt} (dB)	τ^{Opt} (bps/Hz)	P_U^{Opt} (dB)	τ^{Opt} (bps/Hz)
MRC model	6.00	1.96	2.00	2.82
SC model	7.00	1.80	5.00	2.65

Fig. 3. investigates the impact transmit power at user on the system performance. In particular, the MRC scheme always has the best performance, while the SC scheme is slightly inferior, and the performance gap between them disappears as transmit power at user increases to over 10 dB. On the other hand, the SC/MRC scheme with lower number of antennas yields the lowest outage throughput, and as N increases, the performance gap in MRC model becomes more significant. Regarding delay-tolerant transmission mode, this phenomenon clearly indicates that the transmit power at user can cause the similar effect to the system performance as depicted in **Fig. 4**.

In **Fig. 4**, the ergodic throughput survey is conducted versus the transmitted power of user. When the transmit power at user is increasingly set, the ergodic throughput first rises (when

$P_U < 10$ (dB) for $N = 5$ and approximately $P_U < 8$ (dB) for $N = 5$), then throughput decreases. It is evident that the more amount of preset power at user is, the more amount of allocated time fraction for EH is. However, the tradeoff between time used for power transfer phase and channel capacity in information processing phase is need be calculated carefully . The optimal value of user's transmit power and respective ergodic throughput is represented in detail in **Table 3**.

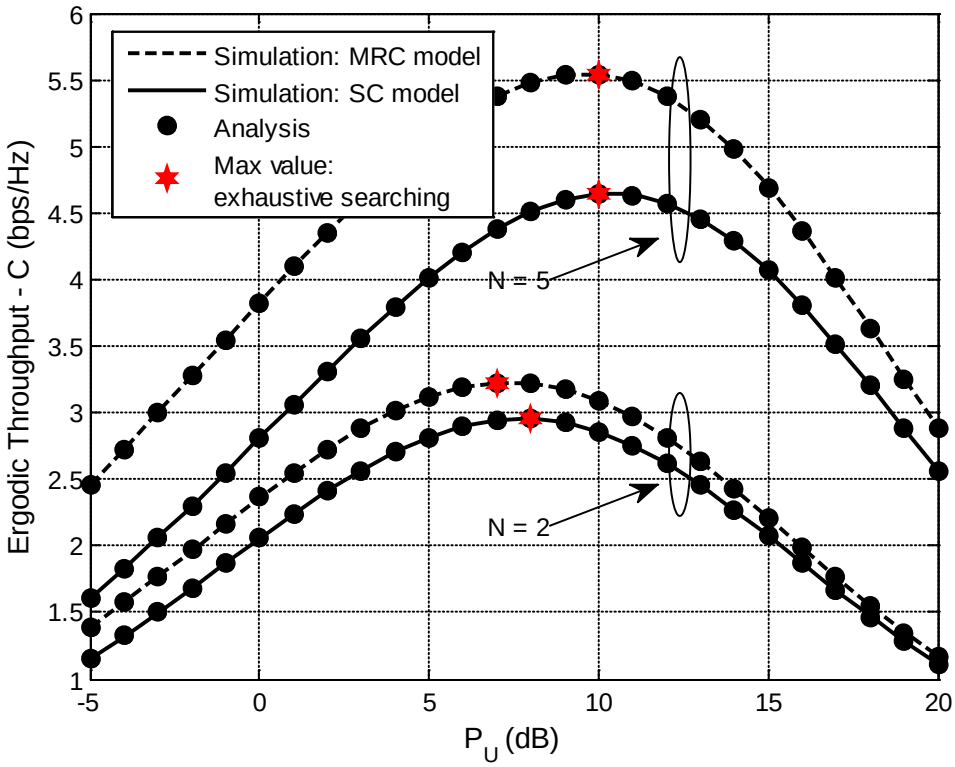

Fig. 4. Ergodic throughput versus transmit power with different combination methods as well as number of AP antennas and $P_{AP} = 10$ (dB).

Table 3. the optimal value of user transmission power and respective ergodic throughput in delay-tolerant tranmission mode.

	$N = 2$		$N = 5$	
	P_U^{Opt} (dB)	C^{Opt} (bps/Hz)	P_U^{Opt} (dB)	C^{Opt} (bps/Hz)
MRC model	7.00	3.23	10.00	5.54
SC model	8.00	2.95	10.00	4.64

4.2 The optimal throughput versus transmission power of AP and comparison experiment

In this experimental simulation, we compare the system performance of wireless energy harvesting using AHTT protocol with those of HTT protocol in [18]. We present the results for the wireless powered with HTT protocol, which serves as a benchmark for performance comparison. It is worth noting that in case of HTT scenario, the SNR at AP node with MRC and SC scheme is given as $\gamma_{MRC}^{HTT} = \frac{\eta\alpha}{1-\alpha}\frac{P_{AP}\|\mathbf{h}_i\|^2\|\mathbf{g}_i\|^2}{d^{2m}\sigma_{AP,i}^2}$ and $\gamma_{MRC}^{HTT} = \frac{\eta\alpha}{1-\alpha}\frac{P_{AP}\|\mathbf{h}_i\|^2}{d^{2m}\sigma_{AP,i}^2}\max\left\{|\mathbf{g}_i|^2\right\}$.

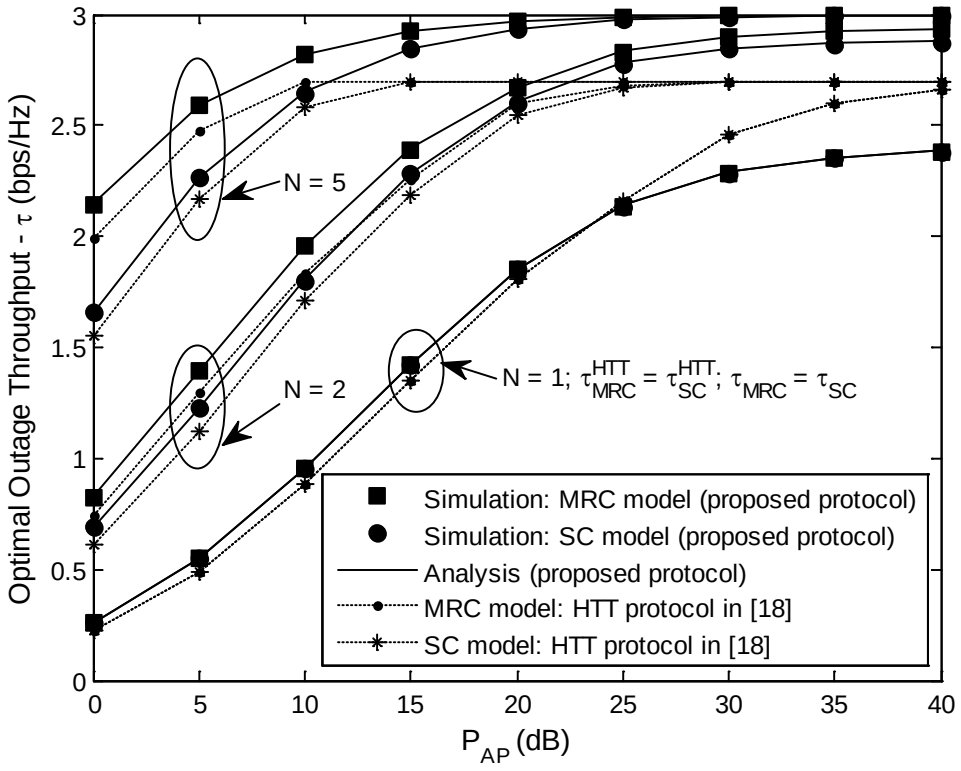

Fig. 5. The optimal outage throughput versus transmit power at AP node with different combination methods and $N \in (1, 2, 5)$ and compared with HTT protocol in [18].

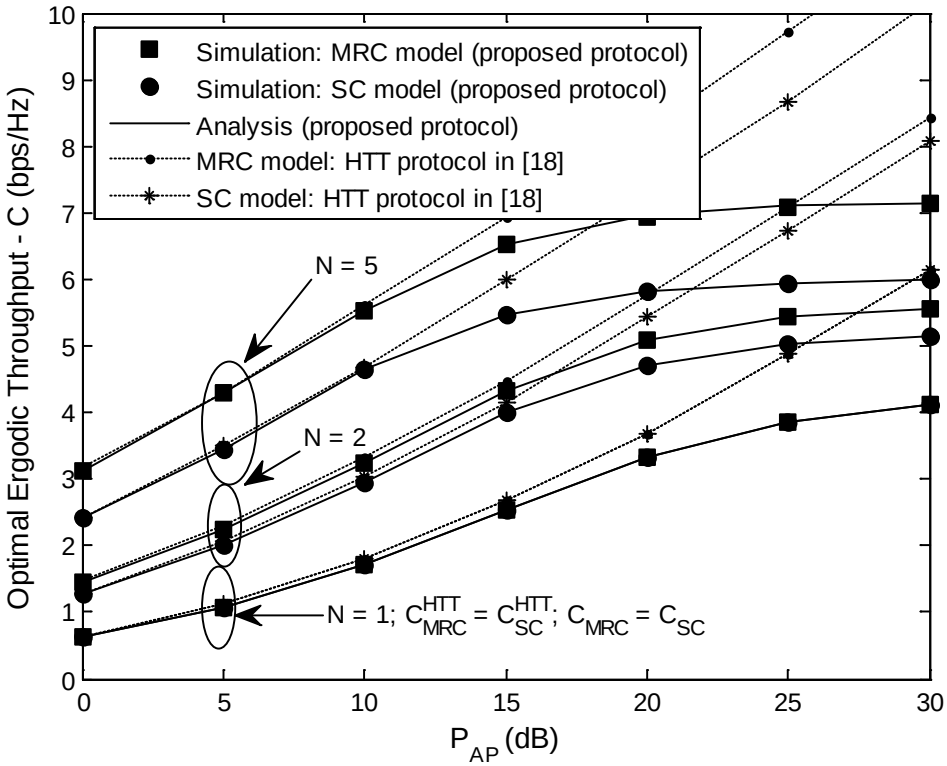

Fig. 6. The optimal ergodic throughput versus transmit power at AP node with different combination methods and $N \in (1, 2, 5)$ and compared with HTT protocol in [18].

In **Fig. 5** and **Fig. 6** show the effect of the transmit power at AP on the system performance. It is noted that **Fig. 5** shows performance for delay-constraint mode while **Fig. 6** illustrates performance for delay-tolerant mode. This observation implies that when increasing the number of antennas more than 2, the quality of multiple-antenna architecture in MISO systems is more significant than that of the MISO with dual antennas. This is quite intuitive since the quality of the system will be improved, if we increase the transmit signal power at AP. In contrast, the quality falls if more energy is harvested at user node.

Fig.5 depicts that although the outage throughput performance of AHTT system outperforms those of HTT, this gap is quite small. The optimal outage first increases when transmit power at H-AP increases, then those values remain stable (at around 3.0 for AHTT protocol and approximate 2.7 (bps/Hz) for HTT strategy, respectively).

As presented in **Fig.6**, the ergodic throughput of HTT climbs sharply when H-AP power increases, while in the proposed AHTT, the throughput rises with the same trend in interval $P_{AP} = [0,15]$ (dB) then slightly increases and stays at the same level of for each scenario (i.e, N = 5, $C \approx 7$ (bps/Hz) for MRC scheme and $C \approx 5.5$ (bps/Hz) for SC system, respectively)

4.3 Throughput versus number of antenna at AP experiment

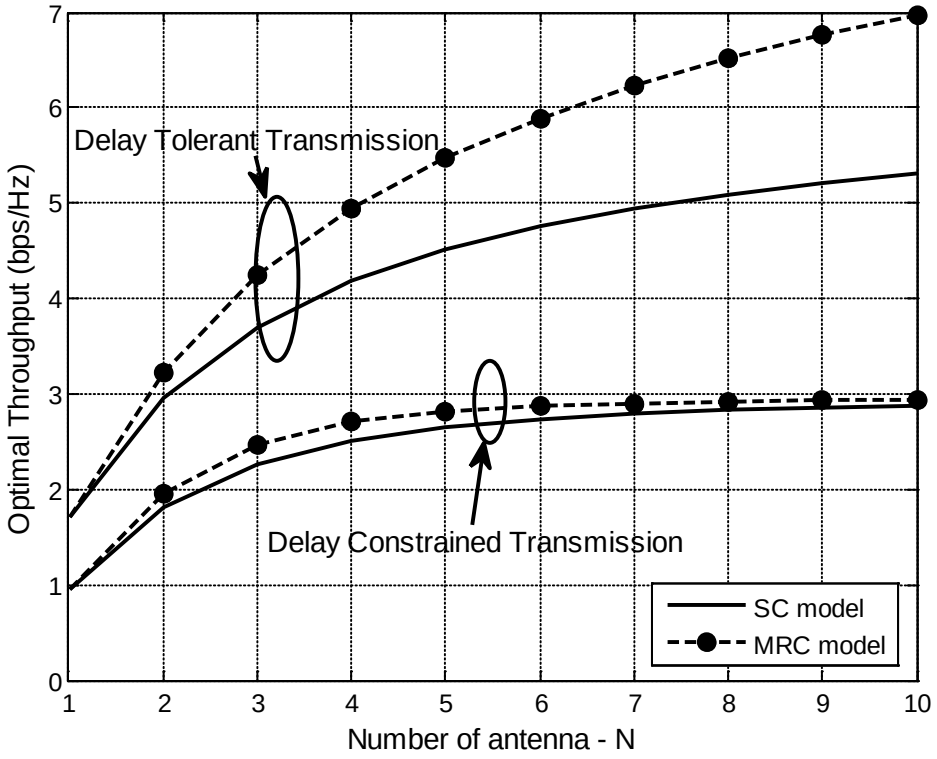

Fig. 7. Optimal throughput versus the number of antennas at the AP with different combination methods and $P_{AP} = 10$ (dB).

Fig. 7 presents the trade-off between the number of antennas at the AP and the system throughput. In particular, the throughput curves of both transmission modes are considered versus the number of antennas for preset values of EH time. At first there is an increase in the system throughput in the delay-constrained mode and then stops at one point as the number of antennas at the AP increases, due to the limitation of the system throughput in this delay-constrained mode, $R(1-\alpha)$. However, when the quantity of antennas becomes larger in the delay-tolerant mode, the system throughput increases. In particular, the throughput performance in the delay-constraint mode is enhanced when the value of throughput climbs from around 1 to approximately 3. There is also a significant increase in the system throughput for delay-tolerant mode.

4. Conclusion

We proposed a new protocol for WPCs so-called AHTT. In this paper, the performance of wireless energy harvesting communication systems with multiple antennas is analyzed. Analytical expressions for the outage probability and ergodic capacity provide a practical insight into the assessment of the system's performance. Furthermore, the optimal transmission power allocation considering the throughput for instantaneous transmission is analytically characterized while the optimal transmit power for both delay-constrained and

delay-tolerant transmission modes are investigated numerically. Numerical results prove that the system throughput in both the delay-constrained and delay-tolerant modes improve, because either the number of antennas or the transmit power of the AP increases then remain unchanged when these two parameters are large enough. Besides that, throughput increases as the perset transmit power of the user increases and then decreases when this power is larger than the optimal value.

Appendix A

This appendix explains for the **Proposition 1** in (12).

Putting $\vartheta = \dfrac{\eta P_{AP,i} \left\| \mathbf{h}_i \right\|^2}{d^m}$ and $\pi = \dfrac{\left\| \mathbf{g}_i \right\|^2}{d^m \sigma_{AP}^2}$, (11) can be rewritten as

$$C_{MRC,i} = \frac{\vartheta}{\vartheta + P_U} \log_2 \left(1 + \pi P_{U,i}\right). \tag{34}$$

Taking the derivative of $C_i\left(P_{U,i}\right)$ with respect to P_U and setting equal zero, we have

$$\pi\vartheta + \pi P_{U,i} = \left(1 + \pi P_{U,i}\right) \ln\left(1 + \pi P_{U,i}\right). \tag{35}$$

After some algebraic manipulations, we obtain

$$\begin{aligned} \frac{\pi\vartheta - 1}{e} &= \frac{1 + \pi P_{U,i}}{e} \ln\left(\frac{1 + \pi P_{U,i}}{e}\right) \\ \Leftrightarrow \frac{\pi\vartheta - 1}{e} &= \exp\left(\ln\left(\frac{1 + \pi P_{U,i}}{e}\right)\right) \ln\left(\frac{1 + \pi P_{U,i}}{e}\right). \end{aligned} \tag{36}$$

Using the form of Lambert W function, (36) can be rewritten as

$$\ln\left(\frac{1 + \pi P_{U,i}}{e}\right) = \mathrm{W}\left(\frac{\pi\vartheta - 1}{e}\right), \tag{37}$$

where $\mathrm{W}(x)$ is the Lambert W function with a solution of $\mathrm{W}(\Omega) = \omega$ is $\omega \exp(\omega) = \Omega$.

After some simple mathematical manipulations, the expression (37) is formulated as

$$P_{U,i}^{opt} = \frac{1}{\pi}\left\{\exp\left[\mathrm{W}\left(\frac{\pi\vartheta - 1}{e}\right) + 1\right] - 1\right\}. \tag{38}$$

This ends the appendix A.

Appendix B

This appendix derives the **Proposition 3**.

Putting $y = \left\| \mathbf{h}_i \right\|^2$ and $x = \left\| \mathbf{g}_i \right\|^2$. Thus, their CDF form is given by [18]

$$F_x(x) = 1 - \exp\left(\frac{-x}{\lambda}\right) \sum_{i=0}^{N-1} \frac{x^i}{i! \lambda^i}. \tag{39}$$

And their probability density function (PDF) form is expressed as

$$f_x(x)=\frac{x^{N-1}}{(N-1)!\lambda^N}\exp\left(\frac{-x}{\lambda}\right). \tag{40}$$

Then (19) is written as

$$\tau_{MRC}=R\times\underbrace{\mathbf{E}_x\left\{\Pr\left\{\frac{P_U x}{d^m\sigma_{AP,i}^2}>\gamma_o\right\}\right\}}_{B}\underbrace{\mathbf{E}_y\left\{1-\frac{P_U d^m}{\eta P_{AP}y+P_U d^m}\right\}}_{A}. \tag{41}$$

The first element in is determined by using the relationship in

$$B=\mathbf{E}_x\left\{\Pr\left(\frac{P_U x}{d^m\sigma_{AP,i}^2}>\gamma_o\right)\right\}=\exp\left(-\frac{d^m\sigma_{AP,i}^2\gamma_o}{P_U\lambda_g}\right)\sum_{i=1}^{N}\frac{1}{(i-1)!}\left(\frac{d^m\sigma_{AP,i}^2\gamma_o}{P_U\lambda_g}\right)^{i-1}. \tag{42}$$

And the second term in (41) is derived as

$$\begin{aligned}A&=\mathbf{E}_y\left\{\frac{\eta P_{AP}y}{\eta P_{AP}y+P_U d^m}\right\}\\&=\frac{\eta P_{AP}}{(N-1)!\lambda_h^N}\int_0^\infty\frac{y^N}{\eta P_{AP}y+P_U d^m}\exp\left(\frac{-y}{\lambda_h}\right)dy\\&=N\left(\frac{P_U d^m}{\eta P_{AP}\lambda_h}\right)^N\exp\left(\frac{P_U d^m}{\eta P_{AP}\lambda_h}\right)\Gamma\left(-N,\frac{P_U d^m}{\eta P_{AP}\lambda_h}\right).\end{aligned} \tag{43}$$

The last integral in (43) is derived by using integral relationship in (eq. 3.383.10) given in [25]. Finally, substituting (42) and (43) into (41), we obtain proposition 3.

Appendix C

This appendix derives the **Proposition 4**.

Putting $z=\max\left(|\mathbf{g}|^2\right)$, the cdf of z is given as

$$F_z(z)=\sum_{p=0}^{N}\binom{N}{p}(-1)^p\exp\left(-\frac{pz}{\lambda}\right). \tag{44}$$

And the PDF of variable z is given by

$$f_z(x)=\frac{N}{\lambda}\sum_{k=1}^{N}\binom{N-1}{k-1}(-1)^{k-1}\exp\left(\frac{-kx}{\lambda}\right). \tag{45}$$

Then, our setting can be shown as

$$\tau_{SC}=R\times\underbrace{\mathbf{E}_z\left\{\Pr\left\{\frac{P_U z}{d^m\sigma_{AP,i}^2}>\gamma_o\right\}\right\}}_{C}\times\underbrace{\mathbf{E}_y\left\{1-\frac{P_U d^m}{\eta P_{AP}y+P_U d^m}\right\}}_{A}. \tag{46}$$

First, with the help of (44), the equivalent of *C* in (46) is evaluated as

$$C = \mathbf{E}_z\left\{\Pr\left\{\frac{P_U z}{d^m \sigma_{AP,i}^2} > \gamma_o\right\}\right\} = 1 - F_z\left(\frac{d^m \sigma_{AP}^2 \gamma_o}{P_U \lambda_g}\right) = 1 - \sum_{p=0}^{N}\binom{N}{p}(-1)^p \exp\left(-\frac{p d^m \sigma_{AP}^2 \gamma_o}{P_U \lambda_g}\right). \quad (47)$$

And the second term in (46) can be derived as in (43). Finally, substituting (43) and (47) into (46), the proposition 4 is derived. This is end of proof.

Acknowledgement

This research is funded by Foundation for Science and Technology Development of Ton Duc Thang University (FOSTECT), website: http://fostect.tdt.edu.vn, under Grant FOSTECT.2016.BR.21

References

[1] A. Kurs, A. Karalis, R. Moffatt, J. D. Joannopoulos, P. Fisher, and M. Soljacic, “Wireless power transfer via strongly coupled magnetic resonances,” *Science*, vol. 137, no. 83, pp. 83–86, Sept. 2007. Article (CrossRef Link).

[2] T. Le, K. Mayaram, and T. Fiez, “Efficient far-field radio frequency energy harvesting for passively powered sensor networks,” *IEEE J. Solid-State Circuits*, vol. 43, no. 5, pp. 1287–1302, May 2008. Article (CrossRef Link).

[3] Dinh-Thuan Do, "Optimal Throughput under Time Power Switching based Relaying Protocol in Energy Harvesting Cooperative Network,” *Wireless Personal Communications*, Vol. 87, No. 2, pp. 551-564, 2016. Article (CrossRef Link).

[4] J. Men, J. Ge and C Zhang, “A joint relay-and-antenna selection scheme in nergy harvesting MIMO relay networks,” *IEEE Signal Processing Letters*, vol. 23, no. 4, pp. 532-536, 2016. Article (CrossRef Link).

[5] Ishibashi, Koji, Hideki Ochiai, and Vahid Tarokh, "Energy harvesting cooperative communications," in *Proc. of Personal Indoor and Mobile Radio Communications (PIMRC), 2012 IEEE 23rd International Symposium on*, pp. 1819-1823. IEEE, 2012. Article (CrossRef Link).

[6] H. Gao, W. Ejaz, and M. Jo, "Cooperative wireless energy harvesting and spectrum sharing in 5G networks," *IEEE Access*, vol. 4, pp. 3647-3658, 2016. Article (CrossRef Link).

[7] R. Rajesh, V. Sharma, and P. Viswanath, “Information capacity of energy harvesting sensor nodes,” in *Proc. of 2011 IEEE International Symposium on Information Theory*, pp. 2363–2367, 2011. Article (CrossRef Link).

[8] H. Lee, K.-J. Lee, H.-B. Kong and I. Lee, "Sum-rate maximization for multiuser MIMO wireless powered communication networks," *IEEE Trans. on Vehicular Technology*, vol. 65, no. 11, pp. 9420-9424, 2016. Article (CrossRef Link).

[9] R. Zhang and C.-K. Ho, “MIMO broadcasting for simultaneous wireless information and power transfer,” *IEEE Trans. Wireless Commun.*, vol. 12, no. 5, pp. 1989–2001, May 2013. Article (CrossRef Link).

[10] Araújo, Daniel C., Taras Maksymyuk, André LF de Almeida, Tarcisio Maciel, João CM Mota, and Minho Jo, "Massive MIMO: survey and future research topics," *Iet Communications* 10, no. 15, p.p. 1938-1946, 2016. Article (CrossRef Link).

[11] X. Ge, R. Zi, H. Wang, J. Zhang, and M. Jo, "Multi-user massive MIMO communication systems based on irregular antenna arrays," *IEEE Transactions on Wireless Communications*, vol. 15, pp. 5287-5301, 2016. Article (CrossRef Link).

[12] F. Rusek *et al.*, “Scaling up MIMO: Opportunities and challenges with very large arrays,” *IEEE Signal Process. Mag.*, vol. 30, no. 1, pp. 40–60, Jan. 2013. Article (CrossRef Link).
[13] L. Lu, G. Y. Li, A. L. Swindlehurst, A. Ashikhin, and R. Zhang, “An overview of massive MIMO: Benefits and challenges,” *IEEE J. Sel. Topics Signal Process.*, vol. 8, no. 5, pp. 742–758, Oct. 2014. Article (CrossRef Link) .
[14] L. Liu, R. Zhang, and K. C. Chua, “Secrecy wireless information and power transfer with MISO beamforming,” *IEEE Trans. Sig. Process.*, vol. 62, no. 7, pp. 1850–1863, Apr. 2014. Article (CrossRef Link).
[15] J. Xu, L. Liu, and R. Zhang, “Multiuser MISO beamforming for simultaneous wireless information and power transfer,” *IEEE Trans. Sig. Process.*, vol. 62, no. 18, pp. 4798–4810, Sept. 2014. Article (CrossRef Link).
[16] C. Shen, W. Li, and T. Chang, “Wireless information and energy transfer in multi-antenna interference channel,” *IEEE Trans. Sig. Process.*, vol. 62, no. 23, pp. 6249–6264, Dec. 2014. Article (CrossRef Link) .
[17] G. Zheng, Z. Ho, E. A. Jorswieck, and B. Ottersten, “Information and energy cooperation in cognitive radio networks,” *IEEE Trans. Sig. Process.*, vol. 62, no. 9, pp. 2290–2303, May 2014. Article (CrossRef Link).
[18] W. Huang, H. Chen, Y. Li, and B. Vucetic, "On the performance of multi-antenna wireless-powered communications with energy beamforming," *IEEE Trans. on Vehicular Technology*, vol. 65, pp. 1801-1808, 2016. Article (CrossRef Link).
[19] Feng, Renhai, Quanzhong Li, Qi Zhang, and Jiayin Qin, "Robust secure transmission in MISO simultaneous wireless information and power transfer system," *IEEE Transactions on Vehicular Technology* 64, no. 1, p. p. 400-405, 2015. Article (CrossRef Link).
[20] C. Xing, N. Wang, J. Ni, Z. Fei, and J. Kuang, “MIMO beamforming designs with partial CSI under energy harvesting constraints,” *IEEE Signal Process. Letters*, vol. 20, pp. 363–366, Apr. 2013. Article (CrossRef Link).
[21] D. W. K. Ng, E. S. Lo, and R. Schober, “Robust beamforming for secure communication in systems with wireless information and power transfer,” *IEEE Trans. Wireless Commun.*, vol. 13, no. 8, pp. 4599-4615, Aug. 2014. Article (CrossRef Link).
[22] S. Leng, D. W. K. Ng, and R. Schober, "Power efficient and secure multiuser communication systems with wireless information and power transfer," in *Proc. of 2014 IEEE International Conference on Communications Workshops (ICC)*, pp. 800-806, 2014. Article (CrossRef Link).
[23] Z. Xiang and M. Tao, “Robust beamforming for wireless information and power transmission,” *IEEE Wireless Commun. Lett.*, vol. 1, no. 4, pp. 372– 375, Aug. 2012. Article (CrossRef Link).
[24] S. Ryhove, G. E. Oien, and L. Lundheim, “An efficient design methodology for constant power link adaptation schemes in short-range scenarios,” *IEEE Trans. Veh. Technol.*, vol. 57, no. 4, pp. 2132–2144, Jul. 2008. Article (CrossRef Link).
[25] Jeffrey, Alan, and Daniel Zwillinger, eds. *Table of integrals, series, and products.* Academic Press, 2007. Article (CrossRef Link).
[26] M Abramowitz, Milton, and Irene A. Stegun. *Handbook of mathematical functions: with formulas, graphs, and mathematical tables*. Vol. 55. Courier Corporation, 1964. Article (CrossRef Link)

Nguyen Xuan-Xinh received his B.S. degree in Electronics and Telecommunications Engineering from Ho Chi Minh University of Technology and Education in 2015. He is currently pursuing his MSc. degree in Telecommunication Engineering at University of Technology, Ho Chi Minh, Viet Nam. His major interests are cooperative (relay) communications, energy harvesting, full-duplex transmission.

Dinh-Thuan Do received the B.S. degree, M. Eng. degree, and Ph.D. degree from Vietnam National University (VNU-HCMC) in 2003, 2007, and 2013 respectively, all in Communications Engineering. He was a visiting Ph.D. student with Communications Engineering Institute, National Tsing Hua University, Taiwan from 2009 to 2010. Prior to joining Ton Duc Thang University, he was senior engineer at the VinaPhone Mobile Network from 2003 to 2009. Dr. Thuan was the recipient of the 2015 Golden Globe Award by Ministry of Science and Technology. He is currently Assistant Professor at the Wireless Communications & Signal Processing Lab (WICOM LAB). His research interest includes signal processing in wireless communications network, mmWave, device-to-device networks, cooperative communications, full-duplex transmission and energy harvesting.